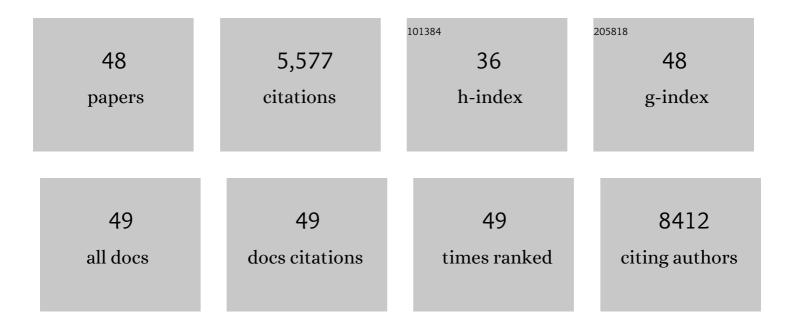
## Junhua Song

List of Publications by Year in descending order

Source: https://exaly.com/author-pdf/10457869/publications.pdf Version: 2024-02-01



LUNHUA SONC

#	Article	IF	CITATIONS
1	Hierarchically Porous M–N–C (M = Co and Fe) Singleâ€Atom Electrocatalysts with Robust MN <i><sub>x</sub></i> Active Moieties Enable Enhanced ORR Performance. Advanced Energy Materials, 2018, 8, 1801956.	10.2	540
2	Extremely Stable Sodium Metal Batteries Enabled by Localized High-Concentration Electrolytes. ACS Energy Letters, 2018, 3, 315-321.	8.8	373
3	Bimetallic Cobaltâ€Based Phosphide Zeolitic Imidazolate Framework: CoP <i><sub>x</sub></i> Phaseâ€Dependent Electrical Conductivity and Hydrogen Atom Adsorption Energy for Efficient Overall Water Splitting. Advanced Energy Materials, 2017, 7, 1601555.	10.2	340
4	Hierarchical porous silicon structures with extraordinary mechanical strength as high-performance lithium-ion battery anodes. Nature Communications, 2020, 11, 1474.	5.8	298
5	Metalâ€Organic Frameworkâ€Derived Nonâ€Precious Metal Nanocatalysts for Oxygen Reduction Reaction. Advanced Energy Materials, 2017, 7, 1700363.	10.2	297
6	Drug-Derived Bright and Color-Tunable N-Doped Carbon Dots for Cell Imaging and Sensitive Detection of Fe <sup>3+</sup> in Living Cells. ACS Applied Materials & amp; Interfaces, 2017, 9, 7399-7405.	4.0	267
7	Selfâ€Assembled Fe–Nâ€Doped Carbon Nanotube Aerogels with Singleâ€Atom Catalyst Feature as Highâ€Efficiency Oxygen Reduction Electrocatalysts. Small, 2017, 13, 1603407.	5.2	254
8	Self-supporting activated carbon/carbon nanotube/reduced graphene oxide flexible electrode for high performance supercapacitor. Carbon, 2018, 129, 236-244.	5.4	244
9	Interphases in Sodiumâ€lon Batteries. Advanced Energy Materials, 2018, 8, 1703082.	10.2	236
10	Graphene Quantum Dot–MnO <sub>2</sub> Nanosheet Based Optical Sensing Platform: A Sensitive Fluorescence "Turn Off–On―Nanosensor for Glutathione Detection and Intracellular Imaging. ACS Applied Materials & Interfaces, 2016, 8, 21990-21996.	4.0	220
11	Efficient Synthesis of MCu (M = Pd, Pt, and Au) Aerogels with Accelerated Gelation Kinetics and their High Electrocatalytic Activity. Advanced Materials, 2016, 28, 8779-8783.	11.1	213
12	A novel approach to synthesize micrometer-sized porous silicon as a high performance anode for lithium-ion batteries. Nano Energy, 2018, 50, 589-597.	8.2	191
13	Metal–organic frameworks-based catalysts for electrochemical oxygen evolution. Materials Horizons, 2019, 6, 684-702.	6.4	149
14	Highly Ordered Mesoporous Bimetallic Phosphides as Efficient Oxygen Evolution Electrocatalysts. ACS Energy Letters, 2016, 1, 792-796.	8.8	139
15	Yolk-shell structured Sb@C anodes for high energy Na-ion batteries. Nano Energy, 2017, 40, 504-511.	8.2	123
16	Ultrafine and highly disordered Ni2Fe1 nanofoams enabled highly efficient oxygen evolution reaction in alkaline electrolyte. Nano Energy, 2018, 44, 319-326.	8.2	118
17	Porous Carbonâ€Hosted Atomically Dispersed Iron–Nitrogen Moiety as Enhanced Electrocatalysts for Oxygen Reduction Reaction in a Wide Range of pH. Small, 2018, 14, e1703118.	5.2	117
18	Enhanced Stability of Li Metal Anodes by Synergetic Control of Nucleation and the Solid Electrolyte Interphase. Advanced Energy Materials, 2019, 9, 1901764.	10.2	108

Junhua Song

#	Article	IF	CITATIONS
19	Lithiumâ€Pretreated Hard Carbon as Highâ€Performance Sodiumâ€Ion Battery Anodes. Advanced Energy Materials, 2018, 8, 1801441.	10.2	105
20	Simultaneous Stabilization of LiNi <sub>0.76</sub> Mn <sub>0.14</sub> Co <sub>0.10</sub> O <sub>2</sub> Cathode and Lithium Metal Anode by Lithium Bis(oxalato)borate as Additive. ChemSusChem, 2018, 11, 2211-2220.	3.6	89
21	Stable Sodium Metal Batteries via Manipulation of Electrolyte Solvation Structure. Small Methods, 2020, 4, 1900856.	4.6	73
22	Optimization of cobalt/nitrogen embedded carbon nanotubes as an efficient bifunctional oxygen electrode for rechargeable zinc–air batteries. Journal of Materials Chemistry A, 2016, 4, 4864-4870.	5.2	72
23	PdCuPt Nanocrystals with Multibranches for Enzyme-Free Glucose Detection. ACS Applied Materials & Interfaces, 2016, 8, 22196-22200.	4.0	68
24	Low Pt-content ternary PdCuPt nanodendrites: an efficient electrocatalyst for oxygen reduction reaction. Nanoscale, 2017, 9, 1279-1284.	2.8	66
25	Optimized Al Doping Improves Both Interphase Stability and Bulk Structural Integrity of Ni-Rich NMC Cathode Materials. ACS Applied Energy Materials, 2020, 3, 3369-3377.	2.5	66
26	Sugar Blowingâ€Induced Porous Cobalt Phosphide/Nitrogenâ€Doped Carbon Nanostructures with Enhanced Electrochemical Oxidation Performance toward Water and Other Small Molecules. Small, 2017, 13, 1700796.	5.2	65
27	Controlling Surface Phase Transition and Chemical Reactivity of O3-Layered Metal Oxide Cathodes for High-Performance Na-Ion Batteries. ACS Energy Letters, 2020, 5, 1718-1725.	8.8	64
28	Three-dimensional PtNi hollow nanochains as an enhanced electrocatalyst for the oxygen reduction reaction. Journal of Materials Chemistry A, 2016, 4, 8755-8761.	5.2	63
29	Multifunctional SnO2/3D graphene hybrid materials for sodium-ion and lithium-ion batteries with excellent rate capability and long cycle life. Nano Research, 2017, 10, 4398-4414.	5.8	63
30	Kinetically Controlled Synthesis of Pt-Based One-Dimensional Hierarchically Porous Nanostructures with Large Mesopores as Highly Efficient ORR Catalysts. ACS Applied Materials & Interfaces, 2016, 8, 35213-35218.	4.0	53
31	Nitrogen and Fluorineâ€Codoped Carbon Nanowire Aerogels as Metalâ€Free Electrocatalysts for Oxygen Reduction Reaction. Chemistry - A European Journal, 2017, 23, 10460-10464.	1.7	52
32	Core–shell PdPb@Pd aerogels with multiply-twinned intermetallic nanostructures: facile synthesis with accelerated gelation kinetics and their enhanced electrocatalytic properties. Journal of Materials Chemistry A, 2018, 6, 7517-7521.	5.2	49
33	Catalytic Activity of Co–X (X = S, P, O) and Its Dependency on Nanostructure/Chemical Composition in Lithium–Sulfur Batteries. ACS Applied Energy Materials, 2018, 1, 7014-7021.	2.5	46
34	Two-Dimensional N,S-Codoped Carbon/Co <sub>9</sub> S <sub>8</sub> Catalysts Derived from Co(OH) <sub>2</sub> Nanosheets for Oxygen Reduction Reaction. ACS Applied Materials & Interfaces, 2017, 9, 36755-36761.	4.0	45
35	A comparative study of pomegranate Sb@C yolk–shell microspheres as Li and Na-ion battery anodes. Nanoscale, 2019, 11, 348-355.	2.8	45
36	Tubular titanium oxide/reduced graphene oxide-sulfur composite for improved performance of lithium sulfur batteries. Carbon, 2018, 128, 63-69.	5.4	43

Junhua Song

#	Article	IF	CITATIONS
37	One-step synthesis of carbon nanosheet-decorated carbon nanofibers as a 3D interconnected porous carbon scaffold for lithium–sulfur batteries. Journal of Materials Chemistry A, 2017, 5, 23737-23743.	5.2	36
38	Template-directed synthesis of nitrogen- and sulfur-codoped carbon nanowire aerogels with enhanced electrocatalytic performance for oxygen reduction. Nano Research, 2017, 10, 1888-1895.	5.8	34
39	Three-dimensional Nitrogen-Doped Reduced Graphene Oxide/Carbon Nanotube Composite Catalysts for Vanadium Flow Batteries. Electroanalysis, 2017, 29, 1469-1473.	1.5	28
40	Assembling Carbon Pores into Carbon Sheets: Rational Design of Three-Dimensional Carbon Networks for a Lithium–Sulfur Battery. ACS Applied Materials & Interfaces, 2019, 11, 5911-5918.	4.0	24
41	Reduction of Nano-Cu <sub>2</sub> O: Crystallite Size Dependent and the Effect of Nano-Ceria Support. Journal of Physical Chemistry C, 2015, 119, 17667-17672.	1.5	23
42	Tuning the structure and composition of graphite-phase polymeric carbon nitride/reduced graphene oxide composites towards enhanced lithium-sulfur batteries performance. Electrochimica Acta, 2017, 248, 541-546.	2.6	20
43	Size dependent compressibility of nano-ceria: Minimum near 33 nm. Applied Physics Letters, 2015, 106, .	1.5	14
44	Self-supporting lithium titanate nanorod/carbon nanotube/reduced graphene oxide flexible electrode for high performance hybrid lithium-ion capacitor. Journal of Alloys and Compounds, 2019, 790, 1157-1166.	2.8	13
45	Enhancing Chemical Interaction of Polysulfide and Carbon through Synergetic Nitrogen and Phosphorus Doping. ACS Sustainable Chemistry and Engineering, 2020, 8, 806-813.	3.2	11
46	Sizeâ€Dependent Crystal Properties of Nanocuprite. International Journal of Applied Ceramic Technology, 2016, 13, 389-394.	1.1	10
47	Insights into the Electrochemical Reaction Mechanism of a Novel Cathode Material CuNi <sub>2</sub> (PO <sub>4</sub> ) <sub>2</sub> /C for Li-Ion Batteries. ACS Applied Materials & Interfaces, 2018, 10, 3522-3529.	4.0	7
48	Water Splitting: Bimetallic Cobaltâ€Based Phosphide Zeolitic Imidazolate Framework: CoP <i><sub>x</sub></i> Phaseâ€Dependent Electrical Conductivity and Hydrogen Atom Adsorption Energy for Efficient Overall Water Splitting (Adv. Energy Mater. 2/2017). Advanced Energy Materials, 2017, 7, .	10.2	1

4